Solid-State Electronics Pergamon Press 1966. Vol. 9, pp. 695–707. Printed in Great Britain

FIELD AND THERMIONIC-FIELD EMISSION IN SCHOTTKY BARRIERS

F. A. PADOVANI and R. STRATTON

Texas Instruments Incorporated, Dallas, Texas, U.S.A.

(*Received* 15 *January* 1966; *in revised form* 18 *February* 1966)

Abstract—Field emission and thermionic-field (T-F) emission are considered as the phenomena responsible for the excess currents observed both in the forward and reverse directions of Schottky barriers formed on highly doped semiconductors. Voltage–current characteristics are derived for field and thermionic-field emission in the forward and reverse regime. The temperatures and voltages where these phenomena are predominent for a given diode are discussed. Comparison with experimental results on GaAs and Si diodes shows good agreement between theory and experiments.

Résumé—On considère l'émission à effet de champ et l'émission thermionique à effet de champ (émission T-F) comme les facteurs responsables pour les surintensités observées dans une barrière de Schottky polarisée en sens direct ou en sens inverse, lorsque cette barrière est formée sur un semi-conducteur fortement dopé. Les caractéristiques courrant–tension sont établies dans le cas de l'émission à effet de champ et de l'émission thermionique à effet de champ pour des polarisations directes et inverses. Les températures où ces effets sont prédominants pour une diode déterminée sont discutées. Une comparaison avec des résultats expérimentaux sur des diodes au silicium et à l'arseniure de gallium montre une très bonne correspondance entre la théorie et l'expérience.

Zusammenfassung—Feldemission und deren Kombination mit thermischer Emission (TF-Emission) sind verantwortlich für den Zusatzstrom in der Vorwärts- und Sperrichtung von Schottky-Übergängen in hochdotierten Halbleitern. Strom–Spannungs-Charakteristiken für Vorwärts- und Sperrichtung werden abgeleitet sowohl für Feldemission als auch für TF-Emission. Es wird diskutiert bei welchen Temperaturen und Spannungen einer gegebenen Diode diese Erscheinungen vorherrschen. Theoretische und experimentelle Ergebnisse für GaAs und Si stimmen gut miteinander überein.

1. INTRODUCTION

SEVERAL authors[1–5] have recently reported departures from the simple diode theory for the forward current characteristic of a metal semiconductor contact. ATALLA and SOSHEA[3] have described their results, by analogy with the case of a p–n junction, in terms of a dimensionless parameter **n**; viz. the forward current is assumed proportional to $\exp(qV/nkT)$ where q is the electronic charge, V the applied voltage, k the Boltzmann's constant and T the absolute temperature. PADOVANI and SUMNER[1] have shown that, in the case of a contact between gold and low-doped gallium arsenide, the observed departures over a wide range of temperatures can be fitted by an expression of the form $\exp[qV/k(T+T_0)]$ where T_0 is a parameter independent of the temperature and voltage.

The diffusion theory for the forward I–V characteristic was reviewed and extended by MACDONALD[7] and STRATTON.[9] Their results indicate that a value of **n**, independent of temperature, equal to 1·06 is appropriate for junctions governed by the diffusion theory.

As a further extension of rectifier theory we have derived the I–V characteristic of a metal semiconductor contact when the impurity concentration in the semiconductor is sufficiently high so as to make field or thermionic-field emission the dominant factor.

The forward and reverse current characteristic of a Schottky barrier will be presented first when

pure field emission dominates and second when thermionic-field emission dominates. The theoretical results will then be compared with our experimental data showing that good agreement exists over a wide range of temperatures. We conclude by drawing some conclusions regarding the use of a Schottky barrier as a hot electron emitter.

2. GENERAL ASSUMPTIONS

Examination of the existing literature shows that field emission and thermionic-field emission calculations readily lead to analytically untractable expressions. Thus, for the sake of mathematical simplicity, a simple potential barrier shape will be assumed. The semiconductor will be assumed to have an impurity concentration, N, independent of temperature and image force correction to the barrier shape will be neglected. For the case of field emission into vacuum the image force leads to correction factors in the transmission probabilities which increase their magnitude but leave their dependence on the field sensibly unaffected over the field range studied. Similarly we believe that for the Schottky barriers, neglect of the image force correction will result in a barrier height, deduced from the I–V characteristic, less than the unmodified actual barrier height. Also, the high energy tail of the derived emitted electron energy distribution will be overestimated near the top of the barrier.

We will also assume that the contribution of the free electrons to the total space charge density is negligible. MACDONALD[7] has shown that this effect is small for non-degenerate material. GOODMAN and PERKINS[8] have derived the influence of this effect on the capacitance of barriers made on degenerate semiconductors and proved it to be quite important. In consequence it appears that this assumption might be more drastic in our case since, as we will see later on, the present calculations apply more especially to the case of highly doped semiconductors.

Under such assumptions, the potential energy, Φ, of the barrier as measured with respect to the energy of the bottom of the conduction band in the bulk of the material is given by[6]

$$\Phi = Nq^2(x-l)^2/2\epsilon, \qquad (1)$$

where x is the distance measured from the metal semiconductor interface, ϵ the dielectric constant of the semiconductor and

$$l = [2\epsilon(E_B - E + \xi_2)/Nq^2]^{1/2} \qquad (2)$$

the width of the space charge region in the semiconductor. Here E_B is the potential energy of the top of the barrier with respect to the Fermi level of the metal, E is the potential energy associated with an applied bias V between the metal and the semiconductor and ξ_2 is the energy of the Fermi level of the semiconductor measured with respect to the bottom of its conduction band.

3. FORWARD VOLTAGE–CURRENT CHARACTERISTIC

For sufficiently thin barriers the major contribution to the forward I–V characteristic is due to electrons tunnelling directly from the conduction band of the semiconductor into the metal.

First, we restrict ourselves to low temperatures where the only contribution to the current arises from electrons tunnelling from the bottom of the conduction band. Next, the calculation is extended to an intermediate temperature range where most of the electrons tunnel at an energy E_m above the conduction band (see Fig. 1) smaller than the

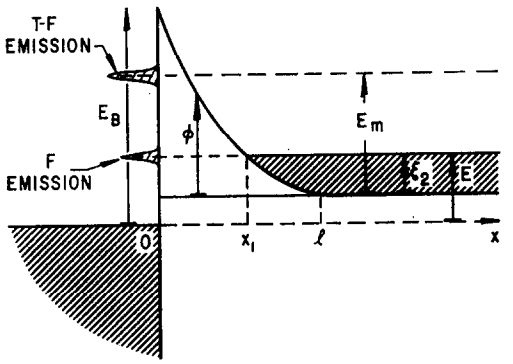

FIG. 1. Electron potential energy diagram of a forward biased Schottky barrier.

energy E_B of the top of the barrier. At even higher temperatures, the main contribution to the current comes from electrons emitted over the top of the barrier. This is the well-known thermionic emission case and the pertinent I–V characteristic can be found in the literature.[6]

Low temperature range

The I–V relationship for field emission at low temperature through an arbitrary potential barrier shape was derived by STRATTON[11] and can be expressed as

$$J = \frac{A \exp -b_1}{(c_1 kT)^2} \frac{\pi c_1 kT}{\sin(\pi c_1 kT)} [1 - \exp(-c_1 V)] \quad (3)$$

where V is the applied bias and

$$A = 4\pi m^* q(kT)^2/h^3 \quad (4)$$

is the classical Richardson constant for the semiconductor under study.[12] The parameters b_1 and c_1, introduced by MURPHY and GOOD,[10] are the first two terms of the Taylor expansion for the exponent of the transparency of the barrier around the Fermi level and can be expressed as

$$b_1 = \alpha \int_{x_1}^{x_2} (\Phi - \xi_2)^{1/2} dx \quad (5)$$

and

$$c_1 = \tfrac{1}{2}\alpha \int_{x_1}^{x_2} (\Phi - \xi_2)^{-1/2} dx. \quad (6)$$

The limits x_1 and x_2 of these integrals are the classical turning points and the constant α is given by

$$\alpha = 2(2m^*)^{1/2}/\hbar. \quad (7)$$

Equation (3) was derived by considering only the first two terms of the Taylor expansion. In consequence, this I–V characteristic will only be valid for temperatures such that[10]

$$1 - c_1 kT > kT(2f_1)^{1/2}. \quad (8)$$

In this inequality f_1 represents the third term of the Taylor expansion of the barrier transparency around the Fermi level and can be expressed as[11]

$$f_1 = \frac{\alpha}{4}\left[\frac{1}{(x_2 - x_1)}\left(\frac{1}{\Phi'(x_1)} - \frac{1}{\Phi'(x_2)}\right)\int_{x_1}^{x_2} \frac{dx}{(\Phi - \xi_2)^{1/2}} - \frac{1}{2}\int_{x_1}^{x_2} \frac{dx}{(\Phi - \xi_2)^{3/2}} \times \left\{1 - \frac{\Phi'(x)}{(x_2 - x_1)}\left(\frac{x - x_1}{\Phi'(x_2)} + \frac{x_2 - x}{\Phi'(x_1)}\right)\right\}\right]. \quad (9)$$

For a Schottky barrier, the constants b_1, c_1 and f_1 can be easily evaluated and the resulting expressions are

$$b_1 = (E_B - E)/E_{00} \quad (10)$$

$$c_1 = [\log\{4(E_B - E)/\xi_2\}]/2E_{00} \quad (11)$$

$$f_1 = \tfrac{1}{4}E_{00}\xi_2. \quad (12)$$

In these expressions E_{00} is an energy given by

$$E_{00} = 2q[N/2\epsilon]^{1/2}/\alpha. \quad (13)$$

For sufficiently large biases, so that $c_1 V \gg 1$, the I–V characteristic can be written as

$$J = J_s \exp(E/E_{00}) \quad (14)$$

where

$$J_s = \frac{2\pi A E_{00} \exp(-E_B/E_{00})}{kT\left[\log\left\{2\left(\frac{E_B - E}{\xi_2}\right)\right\}\right] \sin\left[\frac{\pi kT}{2E_{00}} \log\left\{2\left(\frac{E_B - E}{\xi_2}\right)\right\}\right]}. \quad (15)$$

A plot of the logarithm of the current as a function of the applied bias will yield a straight line of slope q/E_{00}, independent of temperature. At a given bias the saturation current depends on temperature as $\pi c_1 kT/\sin(\pi c_1 kT)$.

For the particular case of a Schottky barrier condition (8) becomes

$$kT < [(2E_{00}\xi_2)^{-1/2} + (2E_{00})^{-1} \log(4E_B/\xi_2)]^{-1}. \quad (16)$$

Intermediate temperature range

Let us now assume that most of the emitted electrons tunnel at an energy E_m smaller than the energy E_B of the top of the barrier, but higher

than the Fermi level energy. Such a case was studied[13] for a potential barrier of arbitrary shape. The I–V relationship could be expressed as

$$J = \frac{A}{2\pi kT}\exp\left(\frac{\xi}{kT} - b_m - \frac{E_m}{kT}\right)\left(\frac{\pi}{f_m}\right)^{1/2} \times [1+\mathrm{erf}(E_m f_m^{1/2})]. \quad (17)$$

The constants b_m, c_m and f_m are now the Taylor expansion coefficients for the exponent of the transparency of the barrier around a particular energy E_m, the position of the peak of the energy distribution of the emitted electrons. This energy E_m will be such that

$$c_m kT = 1. \quad (18)$$

It can also be shown that the energy distribution of the emitted electrons is a Gaussian distribution with half-width[14]

$$\Delta = (\log 2)^{1/2} f_m^{-1/2}. \quad (19)$$

As in the preceeding case these results are only valid in a certain temperature range given by the two conditions

$$c_1 kT > 1 \quad (20)$$

$$D(E_m) < 1/e \quad (21)$$

where $D(E_m)$ is the transparency of the barrier at the energy E_m.[13]

The constants b_m, c_m and f_m are given by expressions analogous to equations (5), (6) and (9) where the Fermi energy ξ_2 has been replaced by the energy E_m and can readily be evaluated in the case of a Schottky barrier. Their values are

$$b_m = \frac{1}{E_{00}}\left[(E_B - E + \xi_2)^{1/2} \times (E_B - E + \xi_2 - E_m)^{1/2} - \frac{E_{00}E_m}{kT}\right] \quad (22)$$

$$c_m = \frac{1}{E_{00}}\log\left[\frac{(E_B - E + \xi)^{1/2} + (E_B - E + \xi - E_m)^{1/2}}{E_m^{1/2}}\right] \quad (23)$$

$$f_m = \cosh^2(E_{00}/kT)/4E_{00}(E_B - E + \xi_2). \quad (24)$$

We can then evaluate the energy E_m by combining equations (18) and (23). The result is

$$E_m = (E_B - E + \xi_2)/\cosh^2(E_{00}/kT). \quad (25)$$

Examination of equation (17) together with the expression for the constants b_m, c_m and f_m reveals that the behaviour of the I–V characteristic will be entirely dominated by the exponential factor. Evaluation of the exponent reveals that

$$b_m + (E_m/kT) = (E_B - E + \xi_2)/E_0 \quad (26)$$

where

$$E_0 = E_{00}\coth(E_{00}/kT). \quad (27)$$

It is again convenient to express the current in term of a saturation current times a voltage dependent term in the following way

$$J = J_s \exp(E/E_0). \quad (28)$$

Neglecting the error function term, the saturation current can be expressed as

$$J_s = \frac{A\pi^{1/2}E_{00}^{1/2}(E_B - E + \xi_2)^{1/2}}{kT\cosh(E_{00}/kT)} \times \exp\left[\frac{\xi_2}{kT} - \frac{E_B + \xi_2}{E_0}\right]. \quad (29)$$

A plot of the logarithm of the current as a function of the applied bias will thus yield a straight line of slope q/E_0. This slope depends on temperature as indicated by equation (27). A normalized plot of such a dependence is shown on Fig. 2.

The above results are only valid in a range of temperatures, given by inequalities (20) and (21). Using equation (11) it is easy to show that the lower temperature limit is such that

$$kT > 2E_{00}\{\log[4(E_B - E)/\xi_2]\}^{-1}. \quad (30)$$

Using for $D(E_m)$ the expression given by STRATTON,[13] one finds that the upper temperature limit [c.f. relation (21)] is given by the condition

$$\cosh^2(E_{00}/kT)/\sinh^3(E_{00}/kT) < 2(E_B + \xi_2 - E)/3E_{00}. \quad (31)$$

The half-width of the electron distribution will be given by

$$\Delta = 2(\log 2)^{1/2}E_{00}^{1/2}(E_B - E + \xi_2)^{1/2}/\cosh(E_{00}/kT). \quad (32)$$

We are now in a position to compare the experimental results with the field or thermionic-field emission equations developed in this section.

Comparison with experimental results

Prior to a detailed analysis of the experimental results, we will consider the orders of magnitude of some of the parameters introduced so far. This will enable us to evaluate, for a given semiconductor, the range of impurity concentrations and temperatures where thermionic-field emission dominates. We will limit our discussion to gold n-type gallium arsenide contacts for which most of our experimental work was done. Identical conclusions can be drawn for any combination of metal and semiconductor of either type provided that appropriate effective mass, barrier height and Fermi energy are chosen.

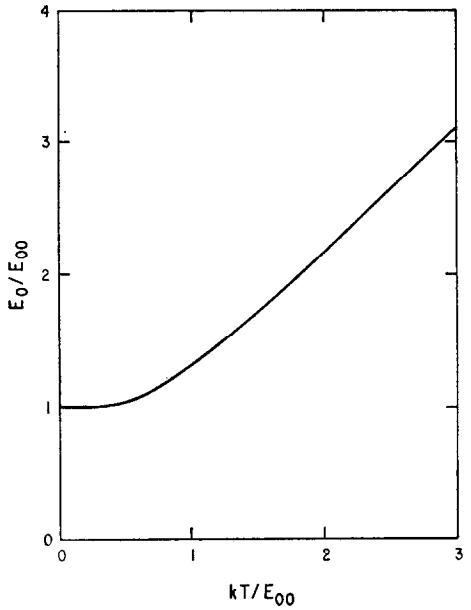

FIG. 2. Normal plot of energy E_0 as a function of reduced temperature.

Let us first consider the upper temperature limit given by relation (31). It is more convenient to discuss it in terms of the maximum bias that can be applied to the junction without making the potential barrier too transparent. This condition is obtained by rewriting equation (31) in terms of the applied bias E

$$E < E_B+\xi_2-\frac{3}{2}E_{00}\frac{\cosh^2(E_{00}/kT)}{\sinh^3(E_{00}/kT)}. \quad (33)$$

Such a relation is represented in Fig. 3 for a barrier height of 0·95 eV typical of gold on gallium arsenide. For a value of E_{00} equal to 15 meV one should observe thermionic-field emission over the whole practical range of temperatures. This value of E_{00} corresponds to a donor concentration of approximately 5×10^{17} atoms cm^3 for n-type gallium arsenide [equation (13)].

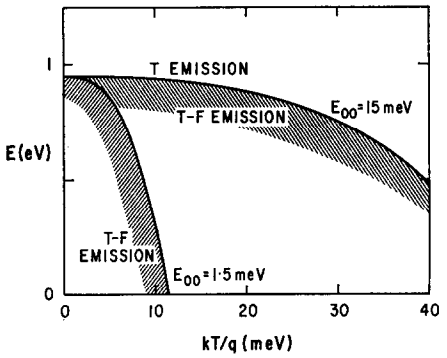

FIG. 3. Maximum forward bias for thermionic-field emission as a function of temperature for different values of the parameter E_{00}.

These results were verified by studying the I–V characteristic of a Schottky barrier made by evaporation of 1000 Å of gold on bulk n-type gallium arsenide with an impurity concentration of 5×10^{17} atoms/cm^3. Details of the measuring techniques have been discussed elsewhere.[1] A typical set of experimental I–V characteristics is shown on Fig. 4. The linear dependence of the logarithm of the current on the applied bias occurs at all temperatures.

The energy E_0 for each temperature can be determined by measuring the slope of the characteristic. Figure 5 is a plot of E_0 as a function of the temperature together with the predicted curve given by equation (27). The value E_{00} was computed for an effective mass of $7\times10^{-2}m_e$ and a carrier concentration of $6{\cdot}5\times10^{17}$ atoms/cm^3 obtained from capacitance measurements (see Fig. 6).

Since the fit obtained in this way between the observed value of E_0 and the computed value is very good we conclude that the forward current of this Schottky barrier is mostly due to thermionic-field emission.

Capacitance measurements for this particular diode shown in Fig. 6 for three temperatures, lead

to an extrapolated barrier height of about 1·10 eV at 0°K. Examination of equation (29) for the saturation current reveals that a plot of the logarithm of $J_s \cosh(E_{00}/kT)/T$ vs. $1/E_0$ should be a straight line of slope $E_B+\xi_2$. Such a plot for the diode under study is shown in Fig. 7 and leads to a barrier height of 1·15 eV in good agreement with the value obtained from capacitance measurements.

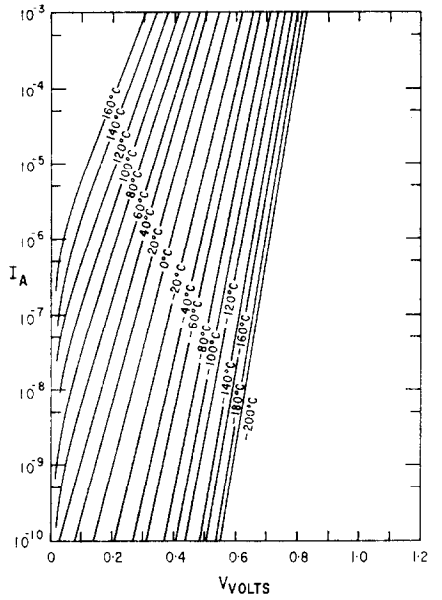

FIG. 4. Forward I–V characteristic of a gold–gallium arsenide Schottky barrier.

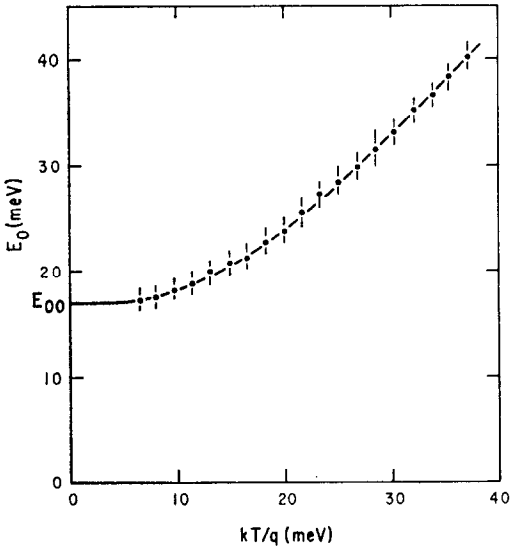

FIG. 5. Experimental values of E_0 as a function of temperature for the diode shown on Fig. 4. The solid line represents the theoretical temperature dependence.

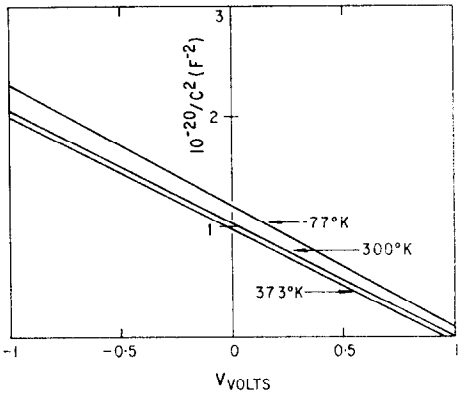

FIG. 6. $1/C^2$ vs. V plot for the gold–gallium arsenide diode.

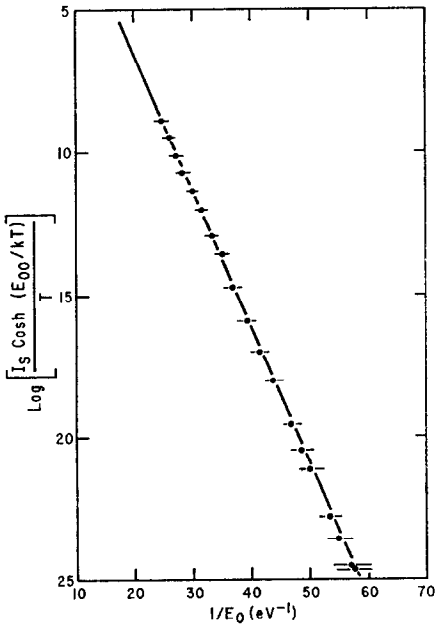

FIG. 7. Saturation current vs. $1/E_0$.

Thus for high concentration materials, conduction properties of a Schottky barrier are dominated by thermionic-field emission. In this process electrons are emitted with a gaussian energy

distribution centred at an energy lower than the energy of the top of the barrier. To illustrate this, a plot of the emitted electron energy distribution for several applied biases is shown on Fig. 8 for room temperature operation and on Fig. 9 for liquid nitrogen operation.

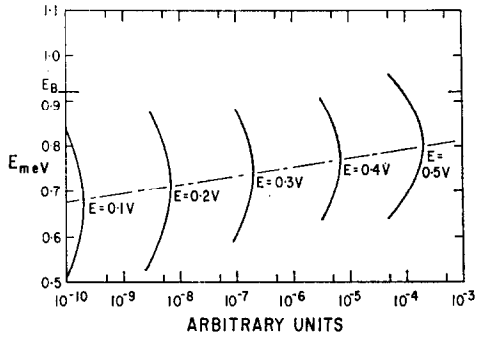

FIG. 8. Emitted electron energy distribution at room temperature for a diode similar to the one studied experimentally.

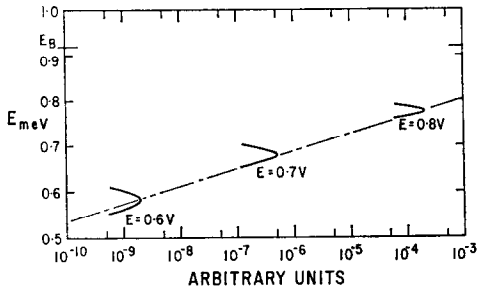

FIG. 9. Emitted electron energy distribution at liquid nitrogen temperature for a diode similar to the one studied experimentally.

4. REVERSE I–V CHARACTERISTIC

We now consider a reverse bias applied to the barrier. This will increase the field in the junction and thus increase the probability for an electron to tunnel from the metal into the semiconductor. If field emission and thermionic-field emission are the dominant forward conduction mechanisms, they will also be the dominant mechanisms for the reverse characteristic.

We will proceed in the same way as for the forward characteristic and divide the temperature range in two parts. First we consider low temperatures where most of the electrons originate from the Fermi level of the metal. Second we consider an intermediate temperature range where the peak of the emitted electrons energy distribution occurs at an energy E_m intermediate between the top of the barrier and the Fermi level of the metal. We will not here consider even higher temperatures where the conduction is controlled by reduction of the barrier height by image force correction. The appropriate characteristics for such a mechanism can be found in the literature.[6]

Low temperature range

The I–V characteristic will again be given by equation (3). The constants b_1, c_1 and f_1 can again be evaluated using equations (5), (6) and (9) with the proper turning points and energies. Figure 10

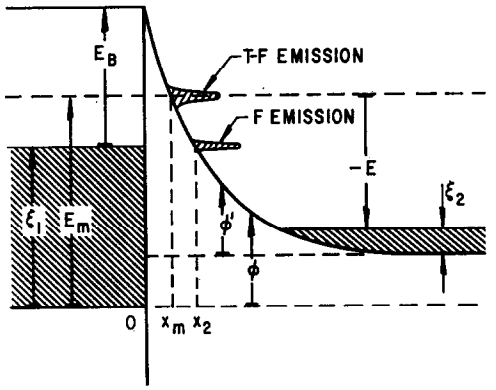

FIG. 10. Electron potential energy diagram of a reverse biased Schottky barrier.

shows an energy diagram of a Schottky barrier under reverse bias conditions and indicates the significance of the different energies involved. Under these conditions

$$b_1 = \frac{1}{E_{00}}\left[E_B^{1/2}(E_B-E)^{1/2}+E \times \log\frac{(E_B-E)^{1/2}+E_B^{1/2}}{(-E)^{1/2}}\right] \tag{34}$$

$$c_1 = \frac{1}{E_{00}}\log\frac{(E_B-E)^{1/2}+E_B^{1/2}}{(-E)^{1/2}} \tag{35}$$

$$f_1 = -\tfrac{1}{2}E_{00}E. \tag{36}$$

In these three expressions E_{00} is the constant defined by equation (13).

Since the expressions for the constants b_1 and c_1 are not very tractable we make certain additional approximations to obtain expressions that can easily be checked experimentally. For example, for reverse biases such that $-E > E_B$, the constants b_1 and c_1 can be approximated by the expressions

$$b_1 = 2E_B^{3/2}/3E_{00}(E_B-E)^{1/2} \quad (37)$$

$$c_1 = E_B^{1/2}/E_{00}(E_B-E)^{1/2}. \quad (38)$$

The resulting I–V characteristic is then

$$J = \frac{A\pi E_{00}\exp[-2E_B^{3/2}/3E_{00}(E_B-E)^{1/2}]}{kT[E_B/(E_B-E)]^{1/2}\sin\{\pi kT[E_B/(E_B-E)]^{1/2}/E_{00}\}} \quad (39)$$

where A is now the Richardson constant for the metal. In the limit of zero temperature, this expression further reduces to

$$J = A\left(\frac{E_{00}}{kT}\right)^2\frac{(E_B-E)}{E_B}\exp\left[-\frac{2E_B^{3/2}}{3E_{00}(E_B-E)^{1/2}}\right]. \quad (40)$$

Equation (40) shows that a plot of the logarithm of $J/(E_B-E)$ as a function of $(E_B-E)^{1/2}$ should yield a straight line of slope $-2E_B^{3/2}/3E_{00}$.

The maximum temperature for which equation (39) is applicable is given by condition (8) where c_1 and f_1 have been replaced by the values obtained from equations (38) and (36). The result is

$$kT < \{E_{00}^{-1}[E_B/(E_B-E)]^{1/2}+(-\tfrac{1}{2}E_{00}E)^{1/2}\}^{-1}. \quad (41)$$

Intermediate temperature range

The constants b_m, c_m and f_m can be evaluated by using equations (5), (6) and (9) with the appropriate turning points and energies. The result is

$$b_m = \frac{(E_m-E-\xi_1)}{E_{00}}\left[\frac{(E_B-E)^{1/2}(E_B+\xi_1-E_m)^{1/2}}{(E_m-E-\xi_1)} - \log\frac{(E_B-E)^{1/2}+(E_B+\xi_1-E_m)^{1/2}}{(E_m-E-\xi_1)^{1/2}}\right] \quad (42)$$

$$c_m = \frac{1}{E_{00}}\log\frac{(E_B-E)^{1/2}+(E_B+\xi_1-E_m)^{1/2}}{(E_m-E-\xi_1)^{1/2}} \quad (43)$$

$$f_m = -\tfrac{1}{4}E_{00}[E-E_B/\cosh^2(E_{00}/kT)]. \quad (44)$$

Using equation (18) we can now derive E_m as a function of the various parameters. After some manipulations the result turns out to be

$$E_m = \xi_1 + \frac{E_B+E\sinh^2(E_{00}/kT)}{\cosh^2(E_{00}/kT)} \quad (45)$$

Once more examination of equation (11) together with the expressions for the constants b_m, c_m and f_m reveals that the behaviour of the I–V characteristic is entirely dominated by the exponential factor.

Evaluation of the exponent shows that

$$\exp\left(\frac{\xi_1}{kT}-b_m-\frac{E_m}{kT}\right) = \exp\left(-\frac{E}{\varepsilon'}-\frac{E_B}{E_0}\right) \quad (46)$$

where

$$\varepsilon' = E_{00}[E_{00}/kT)-\tanh(E_{00}/kT)]^{-1} \quad (47)$$

and

$$E_0 = E_{00}\coth(E_{00}/kT). \quad (48)$$

The I–V relationship can thus be expressed as

$$J = J_s\exp-(E/\varepsilon') \quad (49)$$

where, neglecting the error function term, the saturation current is given by

$$J_s = \frac{A(\pi E_{00})^{1/2}}{kT}\left[-E+\frac{E_B}{\cosh^2(E_{00}/kT)}\right]^{1/2} \times\exp\left(-\frac{E_B}{E_0}\right). \quad (50)$$

These expressions cannot be checked experimentally as easily as in the forward conduction case. The only result that can be easily checked is the exponential dependence of the current on applied bias. The slope of this plot will depend on temperature as indicated by equation (47). A normalized plot of the temperature dependence for the energy ε' is shown on Fig. 11.

The above results are only valid as long as conditions (20) and (21) are fulfilled. Condition (20) will give the limit between the field emission case and the thermionic-field emission case. It can be

easily seen that in the reverse case conditions (20) and (8) give almost the same limit. Figure 12 shows a plot of $1/c_1$ vs. the applied bias E for several values of E_{00} which allows one to determine at a given temperature the applied biases corresponding to thermionic-field emission and field emission.

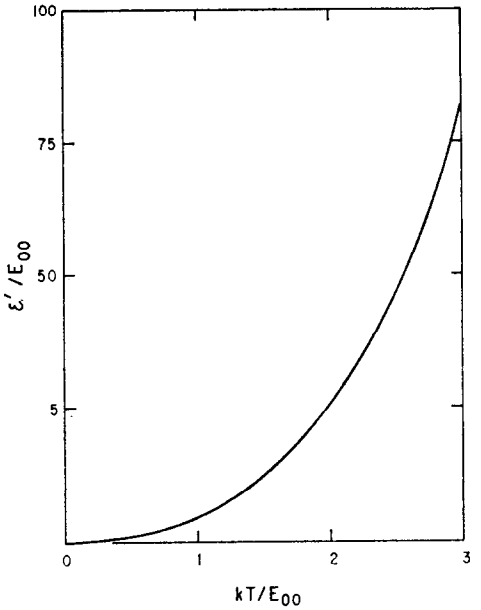

FIG. 11. Normal plot of energy ε' as a function of reduced temperature.

Condition (21) will give the upper temperature limit or the minimum bias to apply to the diode in order to observe thermionic-field emission. Using for $D(E_m)$ the expression given by STRATTON,[11] one finds that the minimum bias to be applied is such that

$$-E > E_B + \frac{3E_{00}}{2}\frac{\cosh^2(E_{00}/kT)}{\sinh^3(E_{00}/kT)}. \qquad (51)$$

Figure 13 shows a plot of this relation for a barrier height of 0·95 eV typical of a gold–gallium arsenide barrier and for several values of E_{00}. Using this plot, one can find at a given temperature the range of bias for which thermionic-field emission occurs.

Finally, the half-width of the emitted electrons distribution will be given by

$$\Delta = 2(\log 2)^{1/2}E_{00}^{1/2}[-E+E_B/\cosh^2(E_{00}/kT)]^{1/2}. \qquad (52)$$

Comparison with experimental results

Examination of Fig. 12 reveals that both regimes can be present at a given temperature depending on the applied bias. This is clearly evidenced on

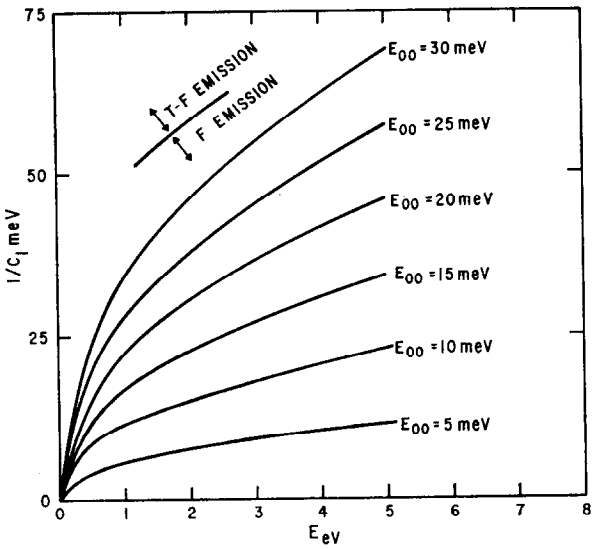

FIG. 12. $1/c_1$ vs. applied bias E plot for several values of the parameter E_{00} and showing for a temperature T the regions of field and thermionic-field emission.

Fig. 14 where the reverse I–V characteristic of the gold–gallium arsenide diode described above is plotted at various temperatures.

For low reverse biases, where thermionic-field emission is predominant, the I–V characteristic is exponential. By measuring the slope of this characteristic, the value of energy ε' at each temperature can be determined. Plotting this energy ε' as a function of kT/q (Fig. 15) shows good agreement between theory and experiment.

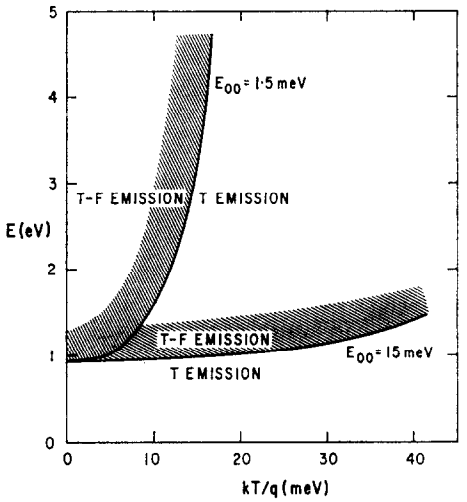

FIG. 13. Minimum reverse bias for thermionic-field emission as a function of temperature for different values of the parameter E_{00}.

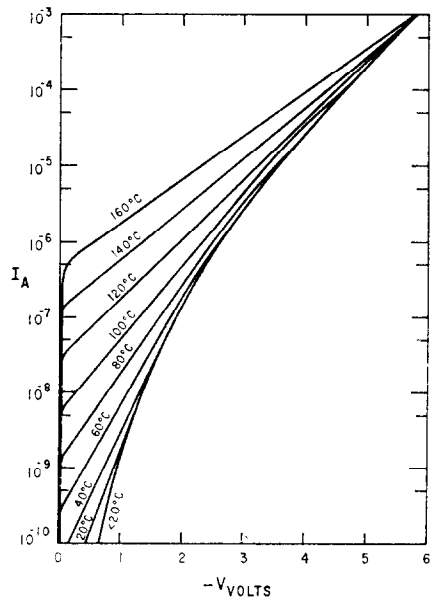

FIG. 14. Reverse I–V characteristic of a gold–gallium arsenide Schottky barrier.

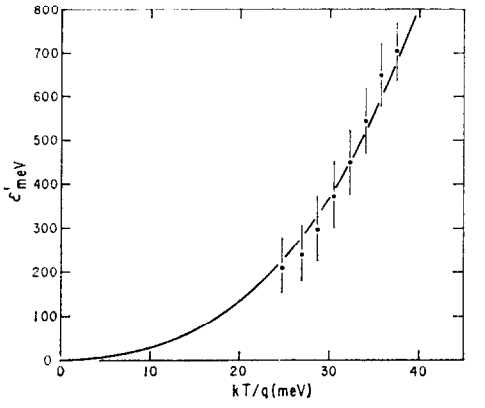

FIG. 15. Experimental values of ε' as a function of temperature for the diode shown on Fig. 14. The solid line represents the theoretical temperature dependence.

Examination of equation (50) reveals that a plot of $\log\{[I_s\cosh(E_{00}/kT)]/T\}$ vs. $1/E_0$ should yield a straight line of slope equal to the barrier height. A value of 1·05 eV can be deduced in this way for the barrier height of this gold–gallium arsenide diode (Fig. 16). Figure 17 shows the energy distribution of the electrons emitted from the metal into the semiconductor as a function of the applied bias for a temperature of 140°C.

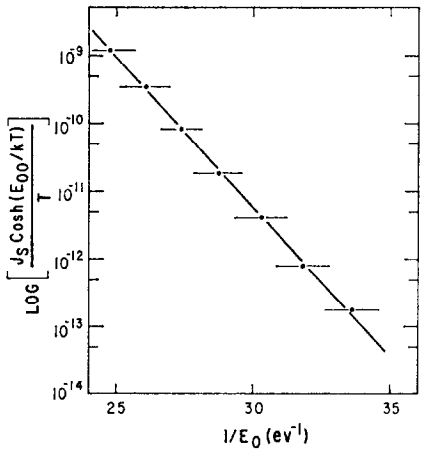

FIG. 16. Reverse saturation current data vs. $1/E_0$.

Pure field emission is more difficult to demonstrate on this particular diode since for the particular parameters of this diode and the temperatures

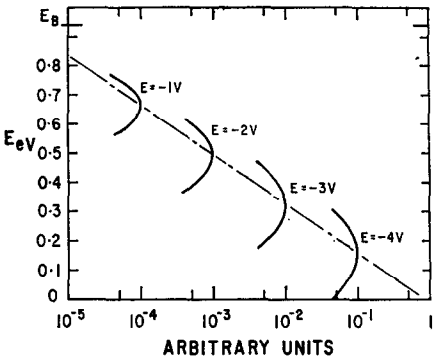

FIG. 17. Emitted electron energy distribution at 140°C for the diode studied experimentally.

studied, equation (39) rather than equation (40) applies. For equation (40) to be a good approximation E_{00} must be increased and the temperature lowered. We used a diode made on n-type silicon with an impurity concentration of 8×10^{18} atoms/cm^3 resulting in a value of E_{00} of 29 meV. Forward and reverse characteristics, measured between 353 and 77°K, are shown in Figs. 18 and 21.

The plot of E_0 (gradient of the logarithm of the forward current vs. the applied bias) vs. kT/q for this diode is shown in Fig. 19 together with the theoretical curve. A plot (Fig. 20) for the saturation current similar to Fig. 7 indicates a barrier height of 0·77 eV in good agreement with the value deduced from capacitance measurements.

The plot of the logarithm of $I/(E_B-E)$ vs. $(E_B-E)^{-1/2}$ for the reverse characteristic at 77°K is shown in Fig. 22 and clearly exhibits a linear dependence over several orders of magnitude. A measure of the slope of the linear region gives a barrier height of 0·79 eV in good agreement with the value deduced from the forward characteristic.

5. CONCLUSIONS

The description of the slope of the forward characteristic for a Schottky barrier in terms of a dimensionless parameter **n** does not give the correct temperature dependence. The use of this parameter is only proper in the case of a p–n junction to describe the influence of space charge recombination effects.[15] The analysis of Schottky barrier data should be made over a wide range of temperatures and plots like the ones shown on Figs. 5 and 18 should be compared with theory. Only then can the conduction mechanism responsible for the observed characteristic be determined and barrier height evaluated. Our study has shown that in the case of Schottky barriers made on highly doped

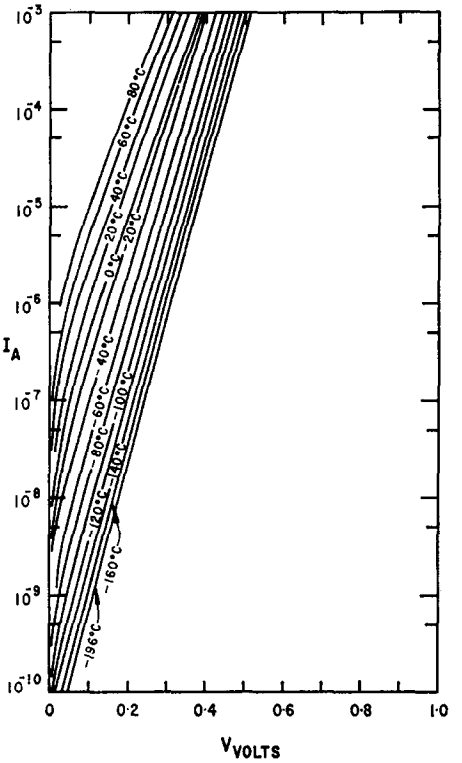

FIG. 18. Forward I–V characteristic of a gold–silicon Schottky barrier.

material (5×10^{16} atoms/cm^3 and above, for gallium arsenide) field emission and thermionic-field emission are the dominant conduction mechanism and that both the reverse and the forward characteristic can be fully explained in this way.

Departures observed[1] in the I–V characteristic of Schottky barriers made on more lightly doped (10^{15} atoms/cm^3) n-type gallium arsenide cannot be explained in this way. We do not at the present time have any explanation for the observed excess temperature T_0 in this case.

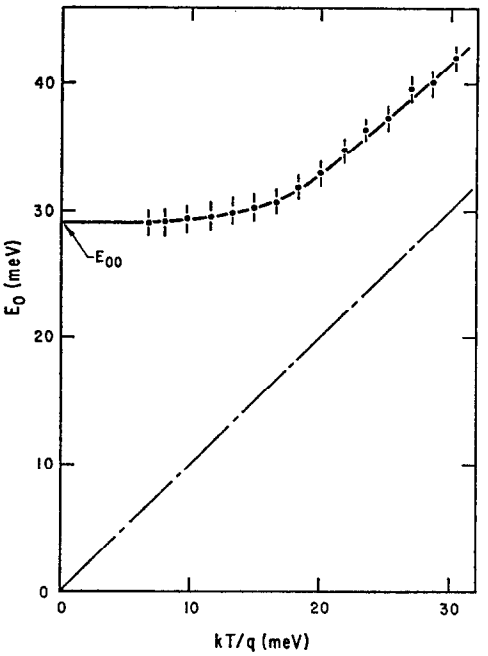

FIG. 19. Experimental values of E_0 as a function of temperature for the silicon diode. The solid line represents the theoretical temperature dependence.

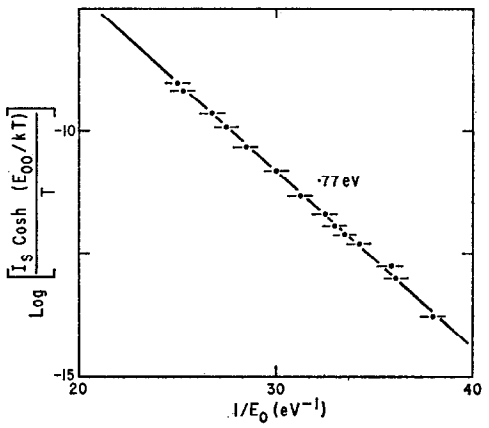

FIG. 20. Saturation current data for the silicon diode as a function of $1/E_0$.

These results have an important bearing in the design of a metal base transistor. In such a structure, a Schottky barrier is used as a hot electron emitter into the metal. Electrons are assumed to be emitted with energy equal to the barrier height and transmission through a thin metal base region

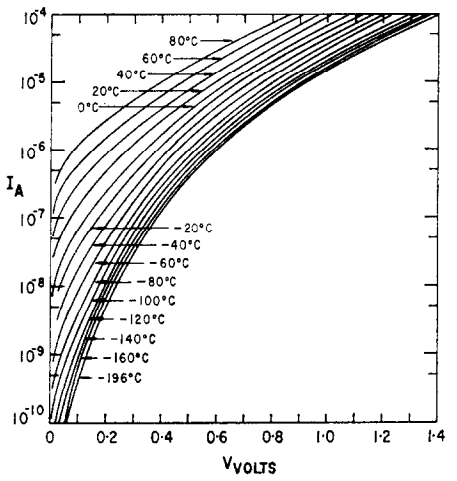

FIG. 21. Reverse I–V characteristic of a gold–silicon Schottky barrier.

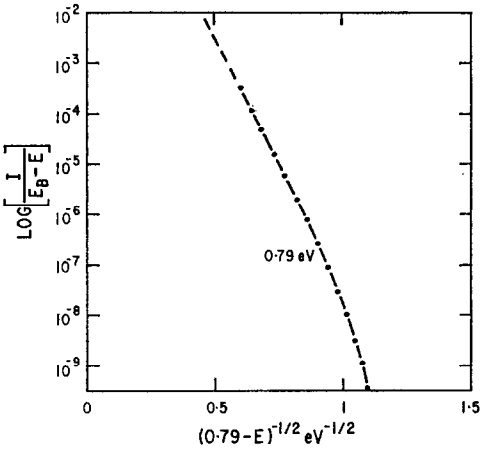

FIG. 22. Logarithm of $I/E_B - E$ vs. $(E_B - E)^{-1/2}$ at liquid nitrogen temperature for the silicon diode.

are collected by a similar barrier. To reduce field emission and thermionic-field emission and thereby improve the emitter efficiency, the emitter diode should be made on a semiconductor with an impurity concentration as low as possible. Alternatively the collector barrier will have to be sufficiently low to collect electrons emitted around the energy E_m.

Acknowledgements—The authors acknowledge with thanks the preparation of the diodes by G. G. SUMNER and W. M. PORTNOY.

REFERENCES

1. F. A. PADOVANI and G. G. SUMNER, *J. appl. Phys.* (to be published).
2. S. M. SZE, C. R. CROWELL and D. KAHNG, *J. appl. Phys.* **35**, 2534 (1964).
3. M. M. ATALLA and R. W. SOSHEA, Scientific Report No. 1 (1962), Contract No. AF 19(628)–1637, Hewlett-Packard Associates.
4. D. KAHNG, *Solid-St. Electron.* **6**, 281 (1963).
5. F. A. PADOVANI, *J. appl. Phys.* (to be published).
6. H. K. HENISH, *Rectifying Semi-conductor Contacts*, Clarendon Press, Oxford (1957).
7. J. R. MACDONALD, *Solid-St. Electron.* **5**, 11 (1962).
8. A. M. GOODMAN and D. M. PERKINS, *J. appl. Phys.* **35**, 3351 (1964).
9. R. STRATTON, *Phys. Rev.* **126**, 2002 (1962).
10. E. L. MURPHY and R. H. GOOD, JR., *Phys. Rev.* **102**, 1464 (1956).
11. R. STRATTON, *J. Phys. Chem. Solids*, **23**, 1177 (1962).
12. C. R. CROWELL, *Solid-St. Electron.* **8**, 395 (1965).
13. R. STRATTON, *Phys. Rev.* **125**, 67 (1962).
14. R. STRATTON, *Phys. Rev.* **135**, 794 (1964).
15. C. T. SAH, R. N. NOYCE and W. SHOCKLEY, *Proc. Inst. Radio Engrs.* **45**, 1228 (1957).